

Cation influence on the structure and electron density of water in some $\text{Me}^{n+} \cdot \text{H}_2\text{O}$ complexes

Kersti Hermansson and Ivar Olovsson

Institute of Chemistry, University of Uppsala, Box 531, S-751 21 Uppsala, Sweden

Sten Lunell

Department of Quantum Chemistry, University of Uppsala, Box 518, S-751 20 Uppsala, Sweden

The cation influence on the water molecule in the $\text{Li}^+ \cdot \text{H}_2\text{O}$, $\text{Be}^{2+} \cdot \text{H}_2\text{O}$, $\text{Mg}^{2+} \cdot \text{H}_2\text{O}$ and $\text{Al}^{3+} \cdot \text{H}_2\text{O}$ complexes has been studied by means of quantum-mechanical *ab initio* calculations. A number of general trends are noted. (1) The calculated equilibrium water O—H distances increase with increasing binding energies, i.e. in the order Li^+ , Mg^{2+} , Be^{2+} , Al^{3+} . The H—O—H angles differ by about $\pm 1^\circ$ from the calculated equilibrium angle for the free H_2O molecule; the variation has no systematic trend. (2) The electron density redistribution accompanying the change in the internal H_2O geometry in these complexes is considerably smaller than the redistribution brought about by the direct influence of the external field. (3) The harmonic O—H stretching force constant decreases with increased cation-water bonding. (4) The qualitative features of the density changes are very similar for the four complexes. The magnitudes of the interactions follow the relation $\text{Li}^+ < \text{Mg}^{2+} < \text{Be}^{2+} \leq \text{Al}^{3+}$. An increased polarization of the H_2O molecule occurs with electron migration from the H atoms towards the O atom and an accumulation of electron charge approximately at the centre of the $\text{Me}^{n+} \text{—O}$ bond, especially in $\text{Be}^{2+} \cdot \text{H}_2\text{O}$ and $\text{Al}^{3+} \cdot \text{H}_2\text{O}$. An electron deficiency is found in the lone-pair region.

Key words: Electron density—Cation-water complexes.

1. Introduction

In a current research project, the structural and electronic characteristics of the water molecule in simple crystalline hydrates have been studied systematically

by both experimental (diffraction, IR, NMR) and theoretical methods. It is relevant in this connection to endeavor to isolate the effect of cation–water interactions for some selected complexes. The results of such calculations are presented here for trigonal $\text{Me}^{n+}\cdot\text{H}_2\text{O}$ complexes for the cations Li^+ , Be^{2+} , Mg^{2+} and Al^{3+} . These cations have been chosen for their different interaction strengths with water. The cation–water interaction has been investigated from three different aspects: the effect on H_2O geometry, the effect on the potential energy surface and the electron redistribution due to the influence of the cation neighbours.

A considerable number of experimental electron density studies of water molecules have been carried out to date by diffraction methods on solid hydrates. About 90% of these water molecules are coordinated to cations, either in an approximately trigonal or tetrahedral bonding situation. Although there is, in these crystalline hydrates, a preference for tetrahedral coordination for monovalent cations (e.g. Li^+), trigonal coordination has been used in all complexes in the present calculations for ease of comparison.

Since the cation–water interaction is important in determining the general chemical behaviour of electrolyte solutions, many theoretical model calculations have already been made. Energy surfaces have been calculated for hydrates of alkali and alkaline–earth metal ions [1–7], as well as hydration shell radii and coordination number [8–9]. Theoretically obtained hydration enthalpies have been compared with experimental values obtained from high-density mass spectrometry [10] or ion cyclotron resonance [11]. Other theoretical studies have addressed themselves to spectroscopic properties of electrolyte solutions [12]. Calculations on complexes between Li^+ and oxygen-containing ligands such as H_2O and H_2CO have also served as model studies for the binding alkali or alkaline–earth ions and ionophores which are organic carriers of cations through membranes [13]. Model calculations on $\text{Zn}^{2+}\cdot\text{H}_2\text{O}$ have helped to elucidate the binding properties of Zn^{2+} , which is an important metal in biological systems [14].

2. Computational method

Ab initio MO-LCAO-SCF calculations have been carried out on the free H_2O molecule and on planar trigonal $\text{Me}^{n+}\cdot\text{H}_2\text{O}$ complexes with $\text{Me}^{n+} = \text{Li}^+$, Be^{2+} , Mg^{2+} and Al^{3+} . The cation–oxygen distances were kept fixed. The potential energy surface for the H_2O molecule was calculated in all cases. The variation of the H_2O geometry for each complex has been indicated in Table 1 together with some other computational details and results. The wave functions were calculated using the program system MOLECULE [15]. The deformation electron density was calculated for each complex in the equilibrium geometry.

2.1. Basis sets

The basis sets consisted of contracted Gaussian type functions of DZP quality or better. The (9s5p/4s) set of Dunning [16] contracted to $\langle 4s2p/2s \rangle$ was used for oxygen and hydrogen, augmented with polarization functions according to

Table 1. Some computational details and results from the calculations on the free H₂O molecule and the four cation-H₂O complexes

	H ₂ O ^a	Li ⁺ ·H ₂ O	Mg ²⁺ ·H ₂ O	Be ²⁺ ·H ₂ O	Al ³⁺ ·H ₂ O
Me ⁿ⁺ -O (Å)	--	1.850	2.050	1.618	1.850
No. of geometries	58	44	30	35	40
O-H range (Å)	0.930-1.025	0.930-1.000	0.930-1.000	0.930-1.000	0.930-1.025
ΔH-O-H range (°)	100.0-110.5	102.0-110.5	100.0-108.5	102.0-110.5	102.5-110.5
Basis sets	O: (9s, 5p, 1d)/(4s, 2p, 1d) H: (4s, 1p)/(2s, 1p)	Li ⁺ : (7s, 1p)/(3s, 1p)	Mg ²⁺ : (10s, 5p)/(5s, 3p)	Be ²⁺ : (7s, 1p)/(3s, 1p)	Al ³⁺ : (10s, 6p)/(5s, 4p)
r _e (Å)	0.94496 (1)	0.95165 (2)	0.96253 (2)	0.97480 (1)	0.99681 (1)
α _e (°)	106.228 (9)	105.924 (8)	105.312 (7)	107.594 (7)	106.396 (8)
Binding energy ^b (kcal/mole)					
V ₀ ^c	-76.046101 (1)	37.7	78.4	135.3	179.1
f _{rr}	9.804 (12)	-83.342295 (1)	-274.754062 (1)	-89.867357 (1)	-316.052618 (1)
f _{αα}	0.851 (3)	9.566 (6)	8.842 (3)	8.066 (6)	6.703 (6)
f _{rr'}	-0.099 (12)	0.908 (2)	0.917 (2)	0.911 (4)	0.882 (2)
f _{rα}	0.242 (2)	0.012 (6)	0.048 (3)	0.067 (6)	0.102 (6)
f _{rr'}	-8.85 (13)	0.181 (1)	0.146 (2)	0.113 (4)	0.114 (2)
f _{ααα}	-0.14 (2)	-9.83 (10)	-9.17 (8)	-9.10 (6)	-9.29 (5)
f _{rrr'}	0.1 (1)	-0.13 (2)	-0.15 (2)	-0.05 (2)	-0.04 (2)
f _{rαα}	-0.02 (7)	0.2 (1)	0.2 (1)	0.0 (1)	0.05 (6)
f _{r'rα}	-0.30 (7)	0.04 (7)	-0.37 (6)	-0.09 (15)	-0.14 (8)
f _{rαα}	-0.21 (2)	-0.23 (7)	-0.32 (6)	-0.56 (15)	0.10 (8)
f _{rαα}		-0.26 (2)	-0.52 (4)	-0.19 (3)	-0.20 (2)

^a The experimental values for the free H₂O molecule are r_e = 0.9572 (3) Å, α_e = 104.52 (5)° [19] and f_{rr} = 8.454, f_{αα} = 0.761, f_{rr'} = -0.101, f_{rα} = 0.228, f_{rrr} = -9.47 (5), f_{ααα} = -0.16 (2), f_{rrr'} = 0.1 (7), f_{rrα} = 0.2(1), f_{r'rα} = -0.4 (3) and f_{rαα} = -0.12 (5) mdyne/Å [38].

^b No correction for zero-point vibrational energy

^c The parameters are listed with reference to the expansion

$$V = V_0 + \frac{1}{2}f_{rr}(\Delta r_1^2 + \Delta r_2^2) + \frac{1}{2}f_{\alpha\alpha}r_e^2\Delta\alpha^2 + f_{rr}\Delta r_1\Delta r_2 + f_{r\alpha}r_e(\Delta r_1 + \Delta r_2)\Delta\alpha + f_{rrr}r_e(\Delta r_1^3 + \Delta r_2^3) + f_{\alpha\alpha\alpha}r_e^2\Delta\alpha^3 + f_{rrr'}r_e \frac{1}{r_e}(\Delta r_1^2\Delta r_2 + \Delta r_1\Delta r_2^2) + f_{rr\alpha}(\Delta r_1^2 + \Delta r_2^2)\Delta\alpha + f_{r'r\alpha}(\Delta r_1\Delta r_2)\Delta\alpha + f_{r\alpha\alpha}r_e(\Delta r_1 + \Delta r_2)\Delta\alpha^2$$

All force constants are in mdyne/Å

Roos and Siegbahn [17], i.e. a set of 3d functions with exponent 1.33 on oxygen and a 2p (0.8) on hydrogen. A scale factor of 1.12 was used for the hydrogen exponent.

For Li^+ the basis set was taken from Clementi and Popkie [3] and the exponent of the 2p polarization function used (0.525) was derived by minimization of the energy of the $\text{Li}^+\cdot\text{H}_2\text{O}$ complex. In the same way, the exponent (0.525) for the polarization function on Be^{2+} was obtained by minimization of the $\text{Be}^{2+}\cdot\text{H}_2\text{O}$ energy. The uncontracted basis functions used for Be^{2+} , Mg^{2+} and Al^{3+} were those of Roos and Siegbahn [18]. For Mg^{2+} the basis set was increased by the addition of a fifth 2p-function with an exponent equal to 0.25. These basis sets were then contracted as indicated in Table 1.

The quality of our basis sets can be judged by comparing the energies given in Table 1 with the energy -76.066 a.u. (approximately 0.002 a.u. above the Hartree-Fock limit) calculated for a free H_2O molecule in the experimental geometry and with a (13s3p3d1f/6s2p1d) basis set [3]. Kistenmacher et al. [5] obtained the energy -83.3575 a.u. for the $\text{Li}^+\cdot\text{H}_2\text{O}$ complex using a (11s7p2d/6s2p/7s2p1d) basis contracted to $\langle 4s3p2d/2s2p/5s2p1d \rangle$ for O/H/ Li^+ (here the Li—O distance was optimized to 1.89 Å and the H_2O geometry was fixed at the experimental values 0.957 Å and 104.5° for the free H_2O molecule [19]).

Test calculations were also carried out for 24 different geometries of the free H_2O molecule with a larger basis set, namely Dunning's (10s6p/5s) set contracted to $\langle 5s3p/3s \rangle$ [20] with one 3d function added on oxygen and one 2p function on hydrogen. The minimum energy decreased from -76.046 to -76.057 a.u. The equilibrium geometry only changed slightly to 0.9419 (3) Å and 106.5(5)°. The harmonic stretching and bending force constants were the same (within one combined standard deviation) as those listed in Table 1. The resulting deformation density maps (Fig. 1a, for example) were almost identical using the two basis sets.

2.2. Choice of metal-oxygen distances

In the present calculations the metal-oxygen distances were not optimized. They were fixed at 1.850, 1.618, 2.050, and 1.850 Å for Li^+ , Be^{2+} , Mg^{2+} and Al^{3+} , respectively.

For $\text{Li}^+\cdot n\text{H}_2\text{O}$ the average Li—O distances obtained from diffraction experiments are approximately 1.96, 2.08 and 2.15 Å for 4-, 5- and 6-coordinated Li^+ ions [21], while no experimental data are available for trigonal coordination. Theoretical *ab initio* calculations on the MO-LCAO-SCF level have given the value 1.89 Å for the Li—O distance in $\text{Li}^+\cdot\text{H}_2\text{O}$ [5], while CI calculations on the same complex by Dierksen, Kraemer and Roos [7] gave a Li—O distance of 1.84 Å.

In the case of Be^{2+} , trigonal coordination has been found in $\text{BeSO}_4\cdot 4\text{H}_2\text{O}$, with a Be—O distance of 1.618 (4) Å. This value was used in the present calculations. It should be remarked, however, that *ab initio* single-determinant SCF calcula-

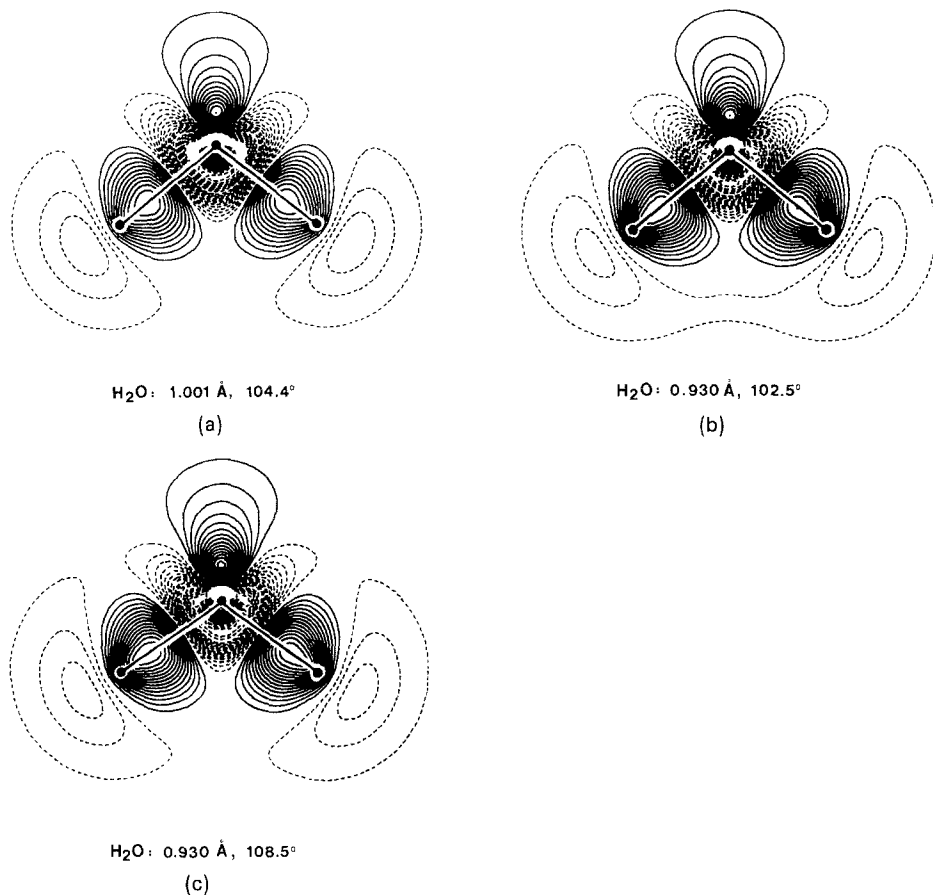


Fig. 1. The deformation electron density, $\rho(\text{H}_2\text{O}) - [\rho(\text{O}) + 2\rho(\text{H})]$, calculated for the free H_2O molecule in some different geometries. Solid lines indicate electron excess, dotted lines electron deficiency. The zero contour is omitted. The contour interval is $\pm 0.05 e \cdot \text{\AA}^{-3}$ ($0.0074 e \cdot \text{a.u.}^{-3}$). The same contour interval is used in all Figs. 1–4. (a) $r(\text{O}-\text{H}) = 1.001 \text{ \AA}$, $\angle \text{H}-\text{O}-\text{H} = 104.4^\circ$ (b) $r(\text{O}-\text{H}) = 0.930 \text{ \AA}$, $\angle \text{H}-\text{O}-\text{H} = 102.5^\circ$ (c) $r(\text{O}-\text{H}) = 0.980 \text{ \AA}$, $\angle \text{H}-\text{O}-\text{H} = 108.5^\circ$

tions as well as CI calculations carried out on $\text{Be}^{2+} \cdot \text{H}_2\text{O}$ by Corongiu and Clementi [22] both gave a shorter Be—O distance, namely 1.54 \AA .

The average Mg—O distance for the octahedrally coordinated water molecules in $\text{MgSO}_4 \cdot 4\text{H}_2\text{O}$ [23] and $\text{MgSO}_4 \cdot 7\text{H}_2\text{O}$ [24] are 2.077 and 2.072 \AA , respectively. Kollman and Kuntz [2] obtained an optimized Mg—O distance of 1.95 \AA in *ab initio* calculations on $\text{Mg}^{2+} \cdot \text{H}_2\text{O}$. The distance 2.05 \AA used here is a compromise between these values.

In a limited literature survey [25] of recently published diffraction studies containing AlO_6 groups seven such groups from four compounds were found, where the standard deviations on the Al—O distances were $\leq 0.01 \text{ \AA}$. In these, the 42 independent Al—O distances were in the range 1.73 – 1.94 \AA with an average value

of 1.88 Å. As a comparison, Kollman and Kuntz [2] obtained a theoretically optimized Al—O distance of 1.75 Å for $\text{Al}^{3+}\cdot\text{H}_2\text{O}$. The value 1.85 Å used here is again a compromise between these values.

3. Results and discussion

3.1. Binding energies

The strengths of the cation-water interaction in the four complexes are distinctly different. As expected, binding energies with respect to dissociation into $\text{Me}^{n+} + \text{H}_2\text{O}$ increase in the order Li^+ , Mg^{2+} , Be^{2+} , Al^{3+} .

Our value for the binding energy of $\text{Li}^+\cdot\text{H}_2\text{O}$ (37.7 kcal/mol) may be compared with the experimental value of 34.1 kcal/mol [10]. Kollman and Kuntz [2] report theoretical binding energies of 37, 80, 140 and 180 kcal/mol for the monohydrates of Li^+ , Mg^{2+} , Be^{2+} and Al^{3+} .

3.2. H_2O geometry

The equilibrium geometry of the free water molecule obtained in our calculations is 0.945 Å for the O—H distance and 106.2° for the H—O—H angle (see Table 1). The best theoretical potential energy surface obtained to date for H_2O from single-determinant SCF calculations has been reported by Rosenberg, Ermler and Shavitt [26]. Their (5s4p2d/3s1p) 39-function STO basis gave an equilibrium geometry of 0.940 Å and 106.1°, and a minimum energy of -76.0646 a.u.

The coordination to Me^{n+} leads to an increase in the O—H distance in the range 0.007–0.052 Å, in the order Li^+ , Mg^{2+} , Be^{2+} , Al^{3+} (Table 1). The H—O—H angles differ by less than 1.4° from the free H_2O value. No particular trend is observed here, however.

Clementi and Popkie [3] optimized the water O—H distance and H—O—H angle both for a free H_2O molecule and for $\text{Li}^+\cdot\text{H}_2\text{O}$ (at an optimized $\text{Li}^+ - \text{O}$ distance of 1.88 Å), and obtained an increase of 0.005 Å in the O—H distance (from 0.950 to 0.955 Å) and a decrease of 0.5° in the angle (from 106.6 to 106.1°) when H_2O binds to Li^+ .

Geometry optimization for an H_2O molecule in a crystalline environment has been carried out for $\text{LiHC}_2\text{O}_4\cdot\text{H}_2\text{O}$ and $\text{NaHC}_2\text{O}_4\cdot\text{H}_2\text{O}$ by Almlöf et al. [27], who found that the O—H distances increased by 0.010–0.025 Å and the H—O—H angle increased by 2.0 and 4.1°.

The average geometry of trigonally coordinated H_2O molecules in crystal hydrates studied by neutron diffraction is 0.980 Å for the O—H distance and 106.8° for the H—O—H angle [28]. The models used most often in the interpretation of diffraction data do not always describe the vibrational motion correctly, however. As a consequence, bias is introduced into the derived H_2O geometry [29]. Such

systematic errors can, in certain cases be as large as $\sim 0.04 \text{ \AA}$ and $\sim 4^\circ$ [30], and thus an order of magnitude larger than the statistical errors for individual diffraction-determined H_2O geometries. Certain general trends can be noted, however. Correlation curves published between quantities such as $\text{O}-\text{H}$ and $\text{O}-\text{H}\cdots\text{O}$ distances [31] clearly indicate that stronger (shorter) hydrogen bonds give rise to longer $\text{O}-\text{H}$ distances. The trend observed in experimental as well as theoretical calculations thus confirms the general expectation that longer $\text{O}-\text{H}$ bonds should arise when the water molecule experiences a stronger polarizing influence from its environment in the form of cation-oxygen contacts and/or hydrogen bonds.

It is more difficult to see general trends in the crystallographic results concerning the variation of the $\text{H}-\text{O}-\text{H}$ angle with different cation-oxygen interaction strength. Even among low-temperature studies where vibrational motion is too small to introduce a significant error into the derived H_2O geometry, examples occur of both larger and smaller $\text{H}-\text{O}-\text{H}$ angles compared to the free H_2O molecule. Moreover, the water H atoms in crystal hydrates are, almost without exception, involved in hydrogen bonding, and it has been found experimentally that there exists a slight correlation between the $\text{H}-\text{O}-\text{H}$ angle and the $\text{X}\cdots\text{O}\cdots\text{Y}$ angle to the acceptors. Such considerations have to be made in comparing theoretically and experimentally obtained geometries.

3.3. Potential energy surfaces

The form of the Taylor expansion for the potential energy surfaces and the calculated coefficients are given in Table 1.

In the present study, the harmonic stretching force constant f_{rr} is seen to decrease with increasing binding energy of the complexes. The stronger bound the complex, the greater is the influence and polarizing effect of the cation on the H_2O molecule. This is consistent with the strong correlation found experimentally between water $\text{O}-\text{H}$ stretching frequency and $\text{O}\cdots\text{O}$ bond distance in crystal hydrates [31]. The coupling force constant $f_{rr'}$ is seen to increase with increasing binding energy for the complexes in Table 1. Fifer and Shiffer [32] have found that the constant $f_{rr'}$ increases with increasing hydrogen bond strength for symmetric water molecules. Eriksson and Lindgren [33] found a linear relationship between f_{rr} and $f_{rr'}$ for the $\text{O}-\text{H}$ stretching vibrations of water molecules in hydrates: $f_{rr'}$ increases as f_{rr} decreases. This trend and its tentative explanation (as given by Fifer and Shiffer [32]) in terms of an enhancement of the effective charge on the water hydrogen atoms are indeed consistent with the results from our calculations (see later for a discussion of the atomic charges).

3.4. Electron density

Difference density maps display the electron redistribution in a system with respect to some reference state such as the superposition of free spherical (or spherically averaged) atoms or ions.

When our attention is focussed on the influence of the surroundings on the electron density of a molecule it would seem natural to choose the density of the free molecule as a reference state. It should be borne in mind, however, that, in addition to the direct influence of the surroundings on the electron distribution in the molecule, the external field brings about a change of the internal molecular geometry – a change which is, in itself, accompanied by an electron redistribution [34].

For practical reasons, the geometries of the water molecules subtracted in the present cases correspond to the bonded situation. Thus, in order for such deformation maps to be a good approximation to the *total* electron redistribution, the electron rearrangement accompanying the *internal* geometry change has to be small. This point is illustrated in Figs. 1a–c, which show the deformation electron density [$\rho(\text{molecule}) - \sum \rho(\text{spherical atoms})$] for H_2O molecules with three different geometries. Indeed, it is seen that for O–H distance variations as large as 0.07 Å and for H–O–H angle variations of the order of 6°, the quantitative density features in Fig. 1, such as O–H bond peak heights, lone-pair peak heights etc., all change by less than 0.15 $e/\text{Å}^3$.

Figs. 2a–d display the difference densities, $\rho(\text{Me}^{n+} \cdot \text{H}_2\text{O}) - [\rho(\text{Me}^{n+}) + \rho(\text{H}_2\text{O})]$, for the cation-water complexes. It is seen that the features in the maps are considerably larger than the effects of the internal geometry change of the H_2O molecule. It is also seen from Fig. 2 that the general features of the electron redistribution are the same regardless of cation. The influence increases in the order Li^+ , Mg^{2+} , Be^{2+} , Al^{3+} , following the order of the binding energies. Moreover, the general features agree very well with the difference map for $\text{Zn}^{2+} \cdot \text{H}_2\text{O}$ calculated by Demoulin and Pullman [14]. These authors also compare the difference density maps for $(\text{H}_2\text{O})_2$ and $\text{Zn}^{2+} \cdot \text{H}_2\text{O}$ and point out the close qualitative similarities between the electron redistribution on hydrogen-bond acceptance and Zn-ligand binding (see also the maps by Morokuma and collaborators [35]). This remark also applies to hydrogen-bond donation [36].

The main influence of the cations on the H_2O electron density is an increased polarity of the molecule, with electron migration from the H atoms towards the O atom. There is an electron deficient region on the cation side of the O atom. This deficiency may in part be due to the charge flow towards the centre of the cation–oxygen bond (cf. Ref. [35]). It may also partly have its origin in the angular redistribution of the electron density around the oxygen atom, i.e. a weakening of the peaks in the lone-pair region as compared to a free H_2O molecule, occurring when the electron charge is pulled along the O–H bonds towards the O atom (cf. the discussions of the deformation density of H_2O in $\text{LiOH} \cdot \text{H}_2\text{O}$ [36] and $\text{NaHC}_2\text{O}_4 \cdot \text{H}_2\text{O}$ [37]). The deformation densities around the two smallest cations have a monopolar character, while for Mg^{2+} and Al^{3+} there is electron excess in the direction towards the oxygen atom and deficiency on the opposite side. One can also see a clear build-up of charge along the metal-oxygen bond in $\text{Be}^{2+} \cdot \text{H}_2\text{O}$ and $\text{Al}^{3+} \cdot \text{H}_2\text{O}$, in contrast to those in the Li^+ and Mg^{2+} complexes (cf. also Ref. [14]).

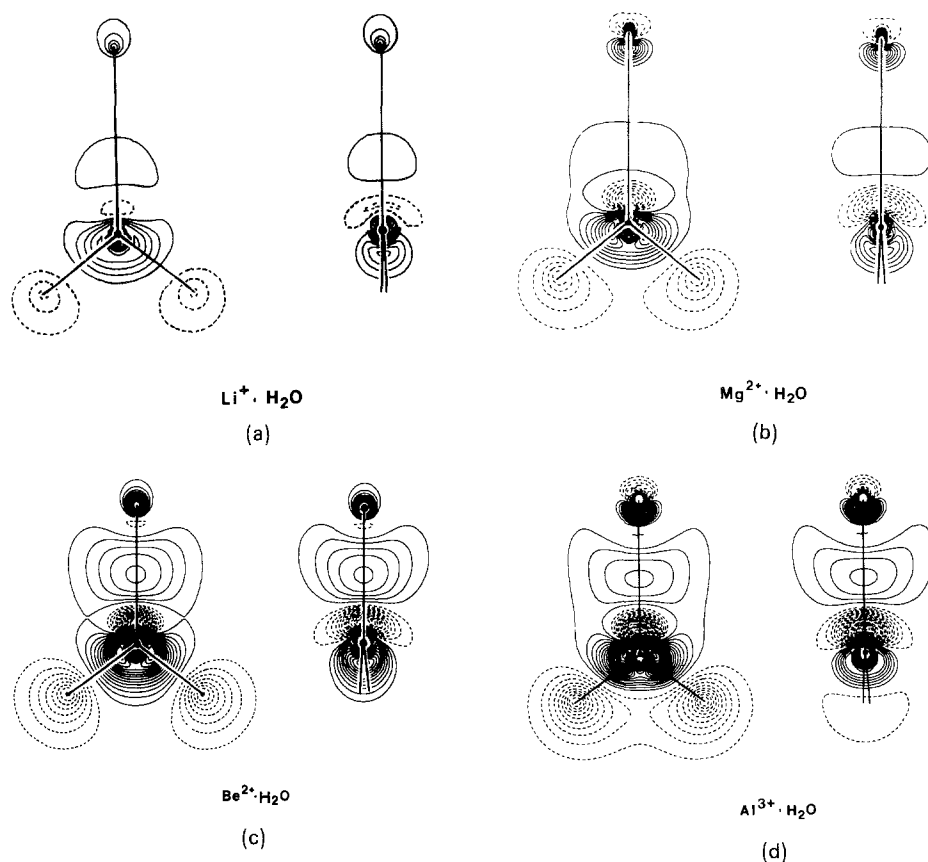


Fig. 2. $\rho(\text{Me}^{n+} \cdot \text{H}_2\text{O}) - [\rho(\text{Me}^{n+}) + \rho(\text{H}_2\text{O})]$ deformation density calculated for some cation-water complexes, where the H_2O geometry has been optimized for a fixed $\text{Me}^{n+} - \text{O}$ distance. (a) $\text{Li}^+ \cdot \text{H}_2\text{O}$; $r(\text{Li}^+ - \text{O}) = 1.850 \text{ \AA}$, $r(\text{O} - \text{H}) = 0.952 \text{ \AA}$, $\angle \text{H} - \text{O} - \text{H} = 105.9^\circ$ (b) $\text{Mg}^{2+} \cdot \text{H}_2\text{O}$; $r(\text{Mg}^{2+} - \text{O}) = 2.050 \text{ \AA}$, $r(\text{O} - \text{H}) = 0.963 \text{ \AA}$, $\angle \text{H} - \text{O} - \text{H} = 105.3^\circ$ (c) $\text{Be}^{2+} \cdot \text{H}_2\text{O}$; $r(\text{Be}^{2+} - \text{O}) = 1.618 \text{ \AA}$, $r(\text{O} - \text{H}) = 0.975 \text{ \AA}$, $\angle \text{H} - \text{O} - \text{H} = 107.6^\circ$ (d) $\text{Al}^{3+} \cdot \text{H}_2\text{O}$; $r(\text{Al}^{3+} - \text{O}) = 1.850 \text{ \AA}$, $r(\text{O} - \text{H}) = 0.997 \text{ \AA}$, $\angle \text{H} - \text{O} - \text{H} = 106.4^\circ$

It has been suggested [14] that the charge depletion close to the oxygen atom is largely a consequence of the repulsive exchange interaction between two closed-shell systems. To test this hypothesis, we replaced the cation by a positive point charge, which obviously cannot involve any exchange interaction. As shown in Fig. 3, the charge rearrangement is very similar to that in the $\text{Li}^+ \cdot \text{H}_2\text{O}$ complex, Fig. 2a. This shows that the charge depletion at the oxygen atom must primarily be a polarization effect.

In order to examine the relative importance of the direct and indirect polarization mechanisms discussed above, calculations were also done for a $\text{Li}^+ \cdot \text{H}_2\text{O}$ complex, with the Li^+ ion displaced out of the plane of the H_2O molecule, Fig. 4. It can be seen that the charge depletion is larger on the side of the oxygen where the Li^+ ion is situated, on account of the electrostatic attraction towards the positive

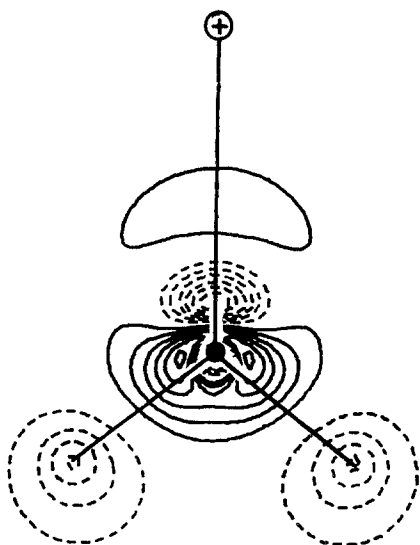


Fig. 3. $\rho(\oplus \cdot \text{H}_2\text{O}) - \rho(\text{H}_2\text{O})$ deformation density. The geometry of the complex was fixed at $r(\oplus - \text{O}) = 1.850 \text{ \AA}$, $r(\text{O} - \text{H}) = 1.001 \text{ \AA}$, $\angle \text{H} - \text{O} - \text{H} = 104.4^\circ$

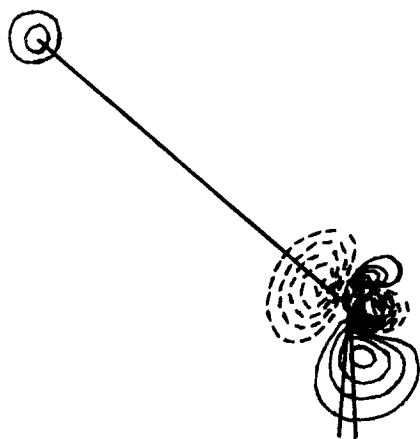


Fig. 4. $\rho(\text{Li}^+ \cdot \text{H}_2\text{O}) - [\rho(\text{Li}^+) + \rho(\text{H}_2\text{O})]$ deformation density for a complex where the Li^+ ion is situated in a plane perpendicular to the water molecular plane. $r(\text{Li}^+ - \text{O}) = 2.000 \text{ \AA}$, $r(\text{O} - \text{H}) = 1.001 \text{ \AA}$, $\angle \text{H} - \text{O} - \text{H} = 104.4^\circ$

ion. Essentially the same picture is obtained if a point charge is used. One can note, however, that the lone pair pointing *away* from the Li^+ ion is also significantly reduced. This decrease must be explained as an indirect effect of the charge displacement towards the oxygen atom in the OH bonds (cf. Refs. [36] and [37]). In general, both polarization mechanisms must therefore be considered.

The charges calculated from the Mulliken population analysis are $-0.52 e$ on O and $+0.26 e$ on H for the free H_2O molecule. The increased polarization due to the presence of Li^+ , Mg^{2+} , Be^{2+} or Al^{3+} are reflected in the O charges which are -0.67 , -0.70 , -0.70 and $-0.76 e$, and the H charges which are $+0.34$, $+0.41$, $+0.46$ and $+0.52 e$ in the different complexes. The cation charges are $\text{Li}^{+0.98}$, $\text{Mg}^{+1.90}$, $\text{Be}^{+1.77}$ and $\text{Al}^{+2.72}$, i.e. the Mulliken population analysis gives charge

transfers of 0.02, 0.10, 0.23 and 0.28 e , respectively. Quantitative significance should naturally not be attached to these numerical values but the general trend is as expected.

4. Concluding remarks

A few points can be made concerning the extension of our results to a more complex bonding situation, such as a crystalline hydrate or an aqueous solution. In such systems, H₂O molecules also participate in hydrogen bonding. As already pointed out, hydrogen bonding to oxygen effects the electron density of the water molecule in a similar way to the effect of coordination to a cation. Thus, the polarity of the bound H₂O molecule increases compared to a non-bonded state both through the cation–water contacts and the hydrogen bonds. On the other hand, the influence of next-nearest neighbours will partly reduce the effect of the nearest neighbours (cf. the theoretical deformation maps for the H₂O molecule in LiOH·H₂O, calculated with and without next-nearest neighbours [36]). Moreover, the cation influence certainly depends on the coordination geometry around the H₂O molecule; the complexes in the present study all have trigonal geometry.

References

1. Diercksen, G. H. F., Kraemer, W. P.: *Theoret. Chim. Acta (Berl.)* **23**, 387–392 (1972)
2. Kollman, P. A., Kuntz, I. D.: *J. Am. Chem. Soc.* **94**, 9236–9237 (1972)
3. Clementi, E., Popkie, H.: *J. Chem. Phys.* **57**, 1077–1094 (1972)
4. Kistenmacher, H., Popkie, H., Clementi, E.: *J. Chem. Phys.* **58**, 1689 (1973)
5. Kistenmacher, H., Popkie, H., Clementi, E.: *J. Chem. Phys.* **58**, 5627 (1973)
6. Kistenmacher, H., Popkie, H., Clementi, E.: *J. Chem. Phys.* **59**, 5842 (1973)
7. Diercksen, G. H. F., Kraemer, W. P., Roos, B. O.: *Theoret. Chim. Acta (Berl.)* **36**, 249–274 (1975)
8. Kollman, P. A., Kuntz, I. D.: *J. Am. Chem. Soc.* **96**, 4766–4769 (1974)
9. Clementi, E., Barsotti, R.: *Chem. Phys. Letters* **59**, 21–25 (1978)
10. Dzidic, J., Kebarle, P.: *J. Chem. Phys.* **74**, 1466 (1970)
11. Beauchamp, J. L.: *Ann. Rev. Phys. Chem.* **22**, 517 (1971)
12. Sadlej, J., Sadlej, A. J.: *J. Chem. Soc. Faraday Discussion.* **64**, 112–119 (1977)
13. Schuster, P., Marius, W., Pullman, A., Berthod, H.: *Theoret. Chim. Acta (Berl.)* **40**, 323–341 (1975)
14. Demoulin, D., Pullman, A.: *Theoret. Chim. Acta (Berl.)* **49**, 161–181 (1978)
15. Almlöf, J.: USIP Report 72-09, University of Stockholm (1972)
16. Dunning, T. H.: *J. Chem. Phys.* **53**, 2823–2833 (1970)
17. Roos, B., Siegbahn, P.: *Theoret. Chim. Acta (Berl.)* **17**, 199–208 (1970)
18. Roos, B., Siegbahn, P.: *Theoret. Chim. Acta (Berl.)* **17**, 209–215 (1970)
19. Benedict, W. S., Gailer, N., Plyler, E. K.: *J. Chem. Phys.* **24**, 1139 (1956)
20. Dunning, T. H.: *J. Chem. Phys.* **55**, 716–723 (1971)
21. Hermansson, K., Thomas, J. O., Olovsson, I.: *Acta Cryst.* **B33**, 2857–2861 (1977)
22. Corongiu, G., Clementi, E.: *J. Chem. Phys.* **69**, 4885–4887 (1978)
23. Baur, W. H.: *Acta Cryst.* **17**, 863–869 (1964)
24. Ferraris, G., Jones, D. W., Yerkess, J.: *J. Chem. Soc. Dalton*, 816–821 (1972)
25. Hermansson, K.: *Acta Cryst.* **C39**, 925–930 (1983)
26. Rosenberg, B. J., Ermler, W. C., Shavitt, J.: *J. Chem. Phys.* **65**, 4072–4080 (1976)

27. Almlöf, J., Lindgren, J., Tegenfeldt, J.: *J. Mol. Struct.* **14**, 427–437 (1972)
28. Chiari, G., Ferraris, G.: *Acta Cryst.* **B38**, 2331–2341 (1982)
29. Cruickshank, D. W. J.: *Acta Cryst.* **9**, 757–758 (1956)
30. Eriksson, A., Berglund, B., Tegenfeldt, J., Lindgren, J.: *J. Mol. Struct.* **52**, 107–112 (1979)
31. Berglund, B.: *Acta Universitatis Upsaliensis, Abs. of Uppsala Diss. from the Faculty of Science*, **448** (1978)
32. Fifer, R. A., Schiffer, J.: *J. Chem. Phys.* **54**, 5097 (1971)
33. Eriksson, A., Lindgren, J.: *J. Mol. Struct.* **53**, 97–102 (1979)
34. Olovsson, I. in: *Electron and magnetization densities in molecules and crystals*, NATO Advanced Study Institute. Series, ed. P. Becker, New York: Plenum Press (1980)
35. Yamabe, S., Morokuma, K.: *J. Am. Chem. Soc.* **97**, 4458–4465 (1975)
36. Hermansson, K., Lunell, S.: *Chem. Phys. Letters* **80**, 64–68 (1981); *Acta Cryst.* **B38**, 2563–2569 (1982)
37. Lunell, S.: *J. Chem. Phys.* to be published
38. Hoy, A. R., Mills, I. M., Strey, G.: *Mol. Phys.* **24**, 1265 (1972)

Received June 8, 1983